EFDA–JET–CP(14)06/26

L. Aho-Mantila, S. Potzel, M. Wischmeier, D.P. Coster, H.W. Müller, S. Marsen, A.G. Meigs, S. Müller, M.F. Stamp, S. Brezinsek, the ASDEX Upgrade Team and JET EFDA contributors

Assessment of Scrape-Off Layer Simulations with Drifts Against L-mode Experiments in ASDEX Upgrade and JET

Assessment of Scrape-Off Layer Simulations with Drifts Against L-mode Experiments in ASDEX Upgrade and JET

L. Aho-Mantila[1], S. Potzel[2], M. Wischmeier[2], D.P. Coster[2], H.W.Müller[2], S. Marsen[3], A.G. Meigs[4], S. Müller[2,5], M.F. Stamp[4], S. Brezinsek[6], the ASDEX Upgrade Team and JET EFDA contributors*

JET-EFDA, Culham Science Centre, OX14 3DB, Abingdon, UK

[1]VTT Technical Research Centre of Finland, Espoo, Finland
[2]Max-Planck-Institut für Plasmaphysik, Garching, Germany
[3]Max-Planck-Institut für Plasmaphysik, Teilinstitut Greifswald, Germany
[4]CCFE Fusion Association, Culham Science Centre, OX14 3DB, Abingdon, OXON, UK
[5]University of California San Diego, US
[6]Institut für Energie- und Klimaforschung - Plasmaphysik, Forschungszentrum Jülich, Germany
** See annex of F. Romanelli et al, "Overview of JET Results", (25th IAEA Fusion Energy Conference, St Petersburg, Russia (2014)).*

Preprint of Paper to be submitted for publication in Proceedings of the 25th IAEA Fusion Energy Conference, St Petersburg, Russia 13th October 2014 - 18th October 2014

ABSTRACT

Numerical simulations of divertor power and particle fluxes in L-mode exhaust scenarios are presented, in comparison to experiments in the full-metal devices ASDEX Upgrade and JET. The simulations are performed using the plasma fluid – Monte Carlo neutrals code package SOLPS5.0, with cross-field drift terms activated. We present a validation of the simulation results against dedicated benchmark experiments with and without nitrogen seeding and discuss the effect of drifts on the modelled divertor asymmetries. At low power dissipation levels, asymmetric divertor conditions are obtained in the simulations as a result of **E×B** drifts, and the modelled volume distributions of particles and energy are largely confirmed by the multiple experimental measurements in both devices. In high-recycling conditions close to the roll-over of the ion fluxes at the target plates, the measured ion fluxes exceed the simulated levels by up to a factor of 6. The discrepancy between the modelled and measured target ion flux evolution is stronger when the divertor conditions are controlled by increasing the deuterium fuelling, in comparison to increasing the impurity-seeding level at constant line-averaged density.

1. INTRODUCTION

Both experimental and analytic considerations have suggested that cross-field drifts (**E×B** and diamagnetic) could significantly modify the power and particle sharing between the divertor legs, therefore influencing the critical power load of the targets and the access to the detached divertor regime required in high-power devices like ITER [1, 2]. Modelling efforts focusing on present-day devices have identified in particular the role of the **E×B** drifts in the divertor asymmetries [3, 4, 5], although contributions arising from **∇B** and curvature drifts have been identified in addition [6]. The **E×B** drifts result from potential variations, which are closely coupled with the radial and poloidal temperature and pressure gradients in the scrape-off layer (SOL) and divertor regions. Therefore, only simulations with self-consistent calculation of the potential distribution and the various divertor plasma-neutral interactions in at least 2 dimensions are conclusive when assessing the effects of drifts on the target power loading.

Good candidates for addressing drift effects are 2D fluid codes, which calculate the drift contributions to the plasma transport, but require input assumptions on SOL power, density and turbulent transport. Several attempts have been made in the past to use experimentally validated fluid simulations to model drift effects, but an unambiguous assessment has been challenging due to lack of global consistency with the diagnostic measurements, see e.g. [7, 8]. In recent years, dedicated L-mode experiments have been carried out in the full-metal tokamaks ASDEX Upgrade and JET to enable further benchmarking of SOL simulationswith drifts. For modelling these experiments we have used the coupled plasma fluid – Monte Carlo neutrals code package SOLPS5.0, which is one of the most widely used 2D simulation tools for calculating the divertor performance and the physical properties of the SOL [9]. The benchmarking of the divertor solutions is summarized in this paper.

The paper is organized as follows. Section 1 describes the modelling approach and discusses the role of drifts in various power exhaust regimes. In Section 2, we present a detailed benchmarking of the low-density divertor solutions against the diagnostic measurements in ASDEX Upgrade. In Section 3, comparison to a similar discharge in JET is presented. In Section 4, benchmarking results for high-recycling divertor conditions are discussed, including N-seeded discharges in both devices. Finally, conclusions and discussion are presented in Section 5.

2. SOLPS5.0 SIMULATIONS OF POWER AND PARTICLE DETACHMENT WITH DRIFTS

The modelling results presented in this contribution follow closely the simulation setup used earlier to model a low-density L-mode discharge in ASDEX Upgrade [10], with the important addition that nitrogen is now included in the solutions for modelling radiative power losses due to seeded impurities [11]. In ASDEX Upgrade, residual N emission is measured also in the absence of seeding and it is taken into account in the simulations, whereas in JET the studied plasmas are assumed to have a negligible fraction of intrisic impurities. In both devices, realistic wall materials are used (but with no sputtering), and full recycling of D and N is assumed at the wall elements (excluding the pumping surfaces).

The benchmarking studies focus on two different exhaust scenarios. First, the evolution of power and particle fluxes is studied in ASDEX Upgrade with increasing D fuelling and, hence, density of the divertor plasma. The modelling study is similar to earlier work [12, 7], but it is shown here as a reference for the quantitative benchmarking presented in the following sections (EDGE2D modelling is being carried out for similar JET experiments [13]). In the second scenario, nitrogen is seeded into the attached, low-recycling conditions in both ASDEX Upgrade and JET, with increasing seeding levels leading to power detachment at the target plates (see the modelling study on the radiative regimes in [14]). The ASDEX Upgrade studies are based on the well-documented L-mode density-ramp Pulse No: 27100 ($B_T = 2.5$T, $I_p = 1.0$MA, $P_{ECRH} = 600$kW) [15]; the steady characterization discharges presented in our paper (Pulse No's: 27688, 27691, 28818) have an identical magnetic configuration. The JET discharges, with a horizontal outer target configuration and various levels of N-seeding ($B_T = 2.5$T, $I_p = 2.5$MA, $P_{NBI} = 1.1$MW, $n_e = 2.7\times10^{19}$ m^{-3}), are documented in [11].

We begin by describing the modelled evolution of the target particle and power fluxes in the different exhaust scenarios, see Fig.1. The analysis assumes diffusive transport coefficients fixed according to measurements in the low-recycling regime ($n_{sep} = 1.2\times10^{19}$ m^{-3} in ASDEX Upgrade, $n_{sep} = 1.6\times10^{19}$ m^{-3} in JET, denoted by red triangles in Fig.1). In both devices, the poloidal variation of the radial transport is enhanced by a ballooning-like rescaling with B−1 dependence. We define the key parameters describing the divertor plasma state as follows. The parallel ion flux density, $\Gamma_{||}$, is the sum of the parallel flux of all ions, weighted by their charge, across a surface perpendicular to the flux tube. The total and peak ion fluxes are denoted by Γ_{tot} and Γ_{pk}, respectively. The parallel power flux, $q_{||}$, includes the kinetic and potential energy of the plasma, and Q_{tot} and Q_{pk} are the

total and peak target power fluxes. Subscripts 'in' and 'out' denote the inner and outer divertor, respectively. The target conditions are defined to be low-recycling when the gradients of electron density, n_e, and temperature, T_e, are small ($n_{pk} \leq 2n_{sep}$ and $T_{e,pk} \geq 0.5T_{e,sep}$), high-recycling when the gradients are large ($n_{pk} \geq 2n_{sep}$ or $T_{e,pk} \leq 0.5T_{e,sep}$), and detached when a significant loss of total pressure, p, is obtained between the target and upstream locations, $p_t \leq 0.1p_{sep}$. The subscript 'sep' refers to the outer midplane separatrix position, whereas 'pk' and 't' refer to the target position.

Figure 1 (a) shows the evolution of the ASDEX Upgrade divertor conditions as a function of n_{sep} in a D-fuelled plasma with no impurities. At low densities ($n_{sep} < 1.8\times10^{19}$ m^{-3}), asymmetries between the two divertors are obtained, as $\Gamma_{tot,in} > \Gamma_{tot,out}$ and $Q_{pk,in} < Q_{pk,out}$. The outer divertor is in the low-recycling regime and the inner divertor is in the high-recycling regime. At around $n_{sep} = 1.8\times10^{19}$ m^{-3}, power detachment and transition to high-recycling regime takes place in the outer divertor, and $\Gamma_{tot,in}$ starts to reduce. At even higher density, $n_{sep} = 2.4\times10^{19}$ m^{-3}, $\Gamma_{tot,out}$ starts to reduce, and the divertor asymmetries change as $\Gamma_{tot,in} < \Gamma_{tot,out}$ and $Q_{pk,in} > Q_{pk,out}$. In comparison to simulations without drifts, which would yield $\Gamma_{tot,out} > \Gamma_{tot,in}$ across the density scan and a symmetric roll-over at $n_{sep} = 2.2\times10^{19}$ m^{-3}, the inclusion of drifts profoundly changes the evolution of the divertor conditions. Only at densities higher than $n_{sep} = 2.6\times10^{19}$ m^{-3}, after the roll-over of both Γ_{tot} and Γ_{pk} at both targets, would a similar evolution be observed in the simulations both with and without drifts.

Figure 1 (b) shows the evolution of the ASDEX Upgrade divertor conditions as a function of increasing N-seeding level at a fixed $n_{sep} = 1.2\times10^{19}$ m^{-3}. Increasing the N concentration in the plasma enhances the power detachment in the inner divertor, reducing $Q_{tot,in}$ and $\Gamma_{tot,in}$. In the outer divertor, a gradual increase of Γ_{pk},out is observed, but the change in $\Gamma_{tot,out}$ is modest. An abrupt reduction of Γ_{tot} is observed at higher seeding levels (3.5×10^{19} at/s) at both targets, accompanied by power detachment and transition to the high-recycling regime at the outer target. This regime covers a rather narrow range of seeding levels, as stronger N seeding leads to unstable solutions (corresponding to plasma disruption). Compared to the smooth evolution of the divertor conditions with increasing D-fuelling, distinct changes are obtained in the target conditions with increasing N-seeding level in the presence of drifts.

Figure 1 (c) shows the evolution of the JET divertor conditions as a function of increasing Nseeding level with a fixed $n_{sep} = 1.6\times10^{19}$ m^{-3}. Similar to ASDEX Upgrade, the initial conditions in JET are very asymmetric with $\Gamma_{tot,in} > \Gamma_{tot,out}$ and $Q_{pk,in} < Q_{pk,out}$. The power detachment occurs simultaneously at both targets (5×10^{19} at/s N-seeding) but, unlike in ASDEX Upgrade, it is followed by an abrupt narrowing of the ion flux profiles and an increase of Γ_{pk} at both targets. The outer divertor evolves from low- to high-recycling regime. Like in ASDEX Upgrade, an abrupt reduction of both Γ_{tot} and Γ_{pk} is obtained simultaneously at both targets at a higher seeding level (2×10^{20} at/s).

Instead of analysing what causes the differences between the different exhaust scenarios, in this paper we focus on the validity of the calculated divertor conditions. Particularly, the level of asymmetry between the two targets, which is profoundly affected by the drifts up to the detachment

of both targets, is benchmarked against experimental measurements. In Sections 3 and 4 the comparisons are shown for conditions in which the outer divertor is in the low-recycling regime (red triangles in Fig.1). In Section 5, the high-recycling conditions are addressed (green triangles in Fig.1).

3. BENCHMARKING THE LOW-DENSITY SOLUTIONS IN ASDEX UPGRADE

First, the divertor conditions at $n_{sep} = 1.2\times10^{19}$ m^{-3} in ASDEX Upgrade are discussed. In Figure 2, the code solutions are compared to the divertor Langmuir probe measurements performed in a recent characterization Pulse No: 27691 ($P_{ECRH} = 400$kW, $n_e = 4.0\times10^{19}$ m^{-3}). The simulations yield an in-out asymmetry at the divertor entrance, with $T_{e,in} < T_{e,out}$ and $\Gamma_{pk,in} > \Gamma_{pk,out}$, arising from the combination of E×B drifts and currents [5]. Because most of the SOL power enters the outer divertor, the resulting conditions are low-recycling, with $T_{e,pk}$ a factor of 8 higher than in the inner divertor. Similar Te measurements by the X-point probe confirm that the parallel Te gradients are small in the outer divertor, as expected in the low-recycling regime. Furthermore, the modelled $\Gamma_{||,out}$ is within the uncertainty range of the X-point measurements, and agrees with the target probe measurements.

A discrepancy is seen, however, when comparing themeasured andmodelled $\Gamma_{||,in}$. The simulations yield a factor of 3 higher $\Gamma_{pk,in}$ than what is measured by the probes. This observation is in line with a two-point model analysis presented in [15], which classifies the inner divertor regime already detached in the experiment. In the simulations, no significant pressure loss is obtained in either divertor leg, which results in an in–out asymmetry in Γ_{tot} that is opposite to the experiments.

The lack of pressure loss in the simulations could mean either deficiencies in modelling the neutral-plasma interaction near the targets, or insufficient accounting of transport processes further upstream, as discussed in [17]. In this regime, X-point probe reciprocations covering the whole divertor volume suffer from an abrupt increase in the measured $\Gamma_{||}$ when crossing the inner separatrix leg, leading to saturation of the signals. This means that the modelled asymmetry in $\Gamma_{||}$ must be valid at least at the entrance to the two divertors. Further information is obtained from the measured Stark broadening of the Balmer line D_δ, which yields a measure for ne in the inner divertor volume [16]. A synthetic diagnostic was implemented in SOLPS5.0 to obtain comparable density evaluations from the simulations. As shown in Figure 3, the Stark broadening measurements are largely in agreement with the simulations, thus confirming the existence of the modelled high-density front in the inner divertor volume (see distribution in [14]). Therefore, it appears likely that the discrepancy with the target $\Gamma_{||}$ results from strong volumetric ion losses just in front of the targets, whereas the modelled in–out asymmetries in the divertor volume, resulting from the drifts, are consistent with the experiments.

4. COMPARISON WITH JET-ILW

The modelled divertor conditions at $n_{sep} = 1.6\times10^{19}$ m^{-3} in JET are compared to Pulse No: 82291. In Figure 4, the SOLPS5.0 solution is compared to the target probe measurements and to the

measured Balmer line emission. In both divertors, the simulations are largely in agreement with the measurements. In particular, $\Gamma_{||}$ in the SOL of the inner divertor, which could not be matched in ASDEX Upgrade, is in satisfactory agreement with the inner target probe measurements. The only notable discrepancies are a small difference between the modelled and measured Te,in, as well as the peak in the inner divertor Balmer line emission at R = 2.4m, which is only obtained in the simulations. This peak is possibly not measured by spectroscopy due to the inner target protrusion at z = –1.5m, or it could be sensitive to the position of the inner strike point, which is uncertain by a few cm. Overall, the modelled in–out asymmetries are in very good agreement with the measurements in this JET discharge, in which the inner divertor is in the high-recycling regime and not yet detached.

5. DISCREPANCIES IN HIGH-RECYCLING CONDITIONS

We turn next to the validation of the simulations when a high-recycling regime is obtained at the outer target. As described in Section 2, this regime is obtained either as a result of increasing D fuelling, or due to seeding of extrinsic impurities. In the simulations, the effects of N seeding are modelled using the same input parameters as in the unseeded cases described in Sections 3 and 4, and solutions that match the measured radiated power (60%) are compared to the experiments. The ASDEX Upgrade discharge with a higher D-fuelling is modelled by raising nsep to 2.2×10^{19} m^{-3}, increasing the input power by 0.2MW, and fitting the transport coefficients to better match the upstream conditions in the corresponding benchmarking Pulse No: 27688 (P_{ECRH} = 600kW, $n_e = 5.7\times10^{19}\ m^{-3}$).

In ASDEX Upgrade, the measured $\Gamma_{pk,\,in}$ reduces with N-seeding, similar to the trend observed in the modelling, see Figure 5(a). Thus, a similar factor of 3 discrepancy is observed between the modelled and measured $\Gamma_{pk,\,in}$ as in the unseeded conditions at $n_{sep} = 1.2\times10^{19}\ m^{-3}$, recall Figure 2. The measured $\Gamma_{pk,\,in}$ increases with increasing D-fuelling, while the changes in the modelled $\Gamma_{pk,\,in}$ are modest, see Figure 5(c). As a result, only 50% discrepancy between the modelled and measured $\Gamma_{pk,\,in}$ is obtained at $n_{sep} = 2.2\times10^{19}\ m^{-3}$. At the outer target, N-seeding reduces the modelled $\Gamma_{pk,\,out}$ but increases the measured $\Gamma_{pk,\,out}$, leading to a factor of 2 discrepancy, see Figure 5(b). The discrepancy at the outer target is, however, much more severe in the case of higher D-fuelling: experimentally, a factor of 6 increase in $\Gamma_{pk,\,out}$ is obtained at $n_{sep} = 2.2\times10^{19}\ m^{-3}$ compared to $n_{sep} = 1.2\times10^{19}\ m^{-3}$, whereas the increase in simulated $\Gamma_{pk,\,out}$ is only about 50%, see Figure 5(d). In JET, N-seeding leads to an increase of Γ_{pk} at both targets, similar to the modelled evolution of Γ_{pk}, see Figure 5(e)–(f). However, at both targets the modelled Γ_{pk} is a factor of 2 smaller than the measured Γ_{pk}.

From these observations we conclude the following. Similar to earlier results [12, 7], the inner target ion fluxes are overestimated by the modelling when the experimental measurements indicate a detached regime in low-density ASDEX Upgrade discharges. This conclusion can be drawn with and without a significant fraction of N impurities in the plasma, i.e., for both low and high radiated power fractions. When the measurements indicate a high-recycling regime in either the outer

or the inner divertor, a smaller Γ_{pk} is modelled than what is measured in both JET and ASDEX Upgrade. The discrepancy is observed to be larger when the high-recycling conditions are obtained by increasing the D-fuelling alone, in comparison to increasing the Nseeding level at low density. Based on the comparisons shown here, the discrepancy between the modelled and measured Γ_{pk} can be quantitatively much larger in the high-recycling conditions than in the detached conditions.

It is worth noting that the discrepancies observed in the D-fuelling scan in ASDEX Upgrade are in line with the observed deviations between the experimental trends and a simple two-point model for the evolution of Γ_{tot} [15]. Future studies should include a careful analysis of the various loss factors (power and momentum losses), which can affect the magnitude of $\Gamma_{||}$.

6 DISCUSSION AND CONCLUSIONS

In the present contribution, it was shown that the divertor power and particle exhaust characteristics can be significantly asymmetric due to cross-field drifts. Furthermore, SOLPS5.0 simulations with drifts were shown to largely reproduce the measured asymmetries in both ASDEX Upgrade and JET under conditions in which the outer divertor is in the low-recycling regime. As concluded in earlier studies [15], the inner divertor of ASDEX Upgrade is in a detached regime already before the roll-over of the ion current, and under these conditions the measured target ion fluxes are overestimated by the simulations by up to a factor of 3, both with and without a significant N impurity concentration. A more significant discrepancy is, however, observed when the outer target (or inner target in JET) enters the high-recycling regime and maximal ion fluxes are measured. In these conditions, the modelling underestimates the ion fluxes by up to a factor of 6. Although more confidence has been obtained about the validity of the drift models included in the SOL simulations, an assessment of the persisting discrepancies should be considered as future work.

ACKNOWLEDGEMENTS

This work was supported by EURATOM and carried out within the framework of the European Fusion Development Agreement and an EFDA Fellowship. The views and opinions expressed herein do not necessarily reflect those of the European Commission.

REFERENCES

[1]. Pitts R et al, 2005 Journal of Nuclear Materials **337-339** 146 – 153
[2]. Chankin A, 1997 Journal of Nuclear Materials **241-243** 199 – 213
[3]. Rozhansky V et al, 2012 Nuclear Fusion **52**(10) 103 017
[4]. Rognlien T D et al, 1999 Physics of Plasmas (1994-present) **6**(5) 1851–1857
[5]. Aho-Mantila L, Coster D andWischmeier M, 2014 In Proc. 41st EPS Conf. on Plasma Physics
[6]. Chankin A et al, 2000 Contributions to Plasma Physics **40**(3-4) 288–294
[7]. Wischmeier M et al, 2011 Journal of Nuclear Materials **415 Supplement** (1) S523 – S529
[8]. Chankin A V et al, 2006 Plasma Physics and Controlled Fusion **48** 839–868

[9]. Schneider R et al, 2006 Contribution to Plasma Physics **46**(1-2) 3–191
[10]. Aho-Mantila L et al, 2012 Nuclear Fusion **52**(10) 103 006
[11]. Aho-Mantila L et al, 2013 Journal of Nuclear Materials **438**, **Supplement (0)** S321 – S325
[12]. Wischmeier M et al, 2009 Journal of Nuclear Materials **390-391** 250 – 254
[13]. Groth M et al, 2014 In Proc. 25th IAEA Fusion Energy Conference
[14]. Aho-Mantila L et al, 2014 Journal of Nuclear Materials submitted
[15]. Potzel S et al, 2014 Nuclear Fusion **54**(1) 013 001
[16]. Potzel S et al, 2014 Plasma Physics and Controlled Fusion **56**(2) 025 010
[17]. Wischmeier M et al, 2012 In Proc. 24th IAEA Fusion Energy Conference

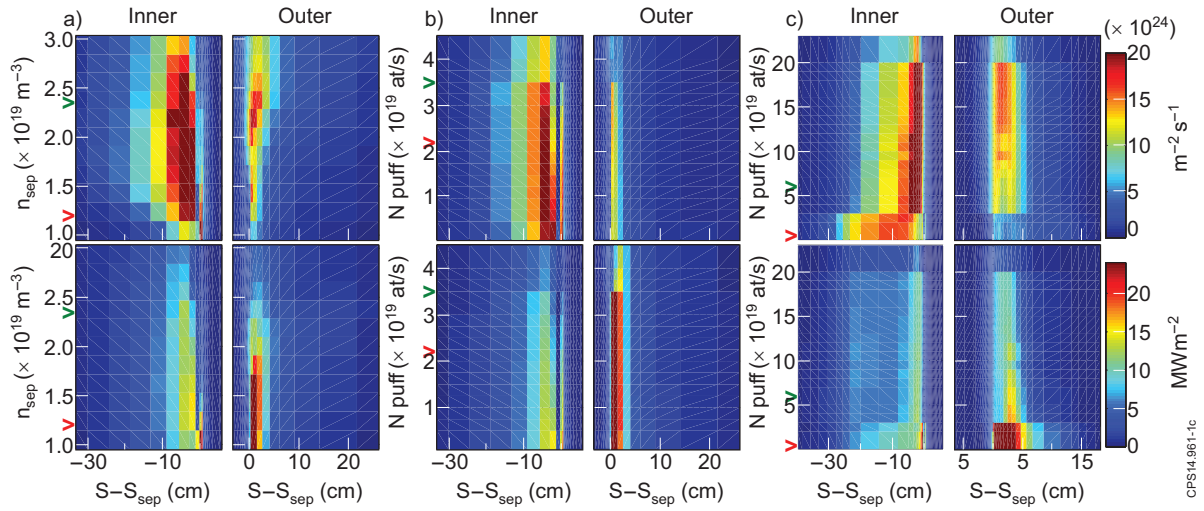

Figure 1: Ion fluxes (top) and heat fluxes (bottom) along the two targets in ASDEX Upgrade (a)–(b) and JET (c). The trends are shown as a function of increasing separatrix density (a) and N-seeding rate (b)–(c). In the seeding scans, nsep is fixed to 1.2×10^{19} m^{-3} (b) and 1.6×10^{19} m^{-3} (c). All input parameters, such as anomalous transport, are adjusted according to the Pulse No: 27691 in ASDEX Upgrade and Pulse No: 82291 in JET (see Sections 3 and 4).

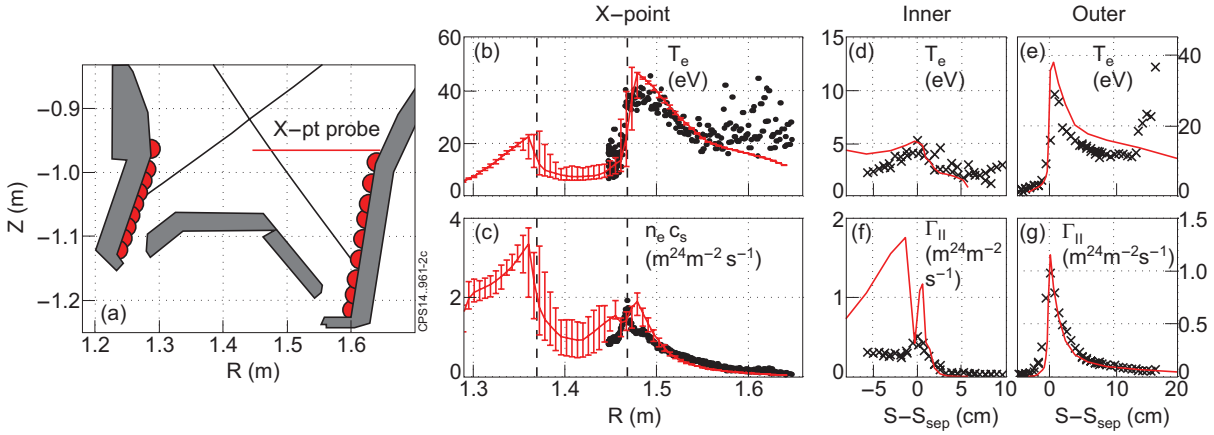

Figure 2: X-point and target probe geometry in ASDEX Upgrade Pulse No: 27691 (a). The thick line shows the maximum range of the X-point probe measurements. Comparison between the simulated (red lines) and measured profiles (black markers) of T_e (top row) and ion fluxes (bottom row) is shown in figures (b)-(c) for the X-point location, in figures (d) and (f) for the inner target and in figures (e) and (g) for the outer target. The coordinate S measures the poloidal distance along the target surface.

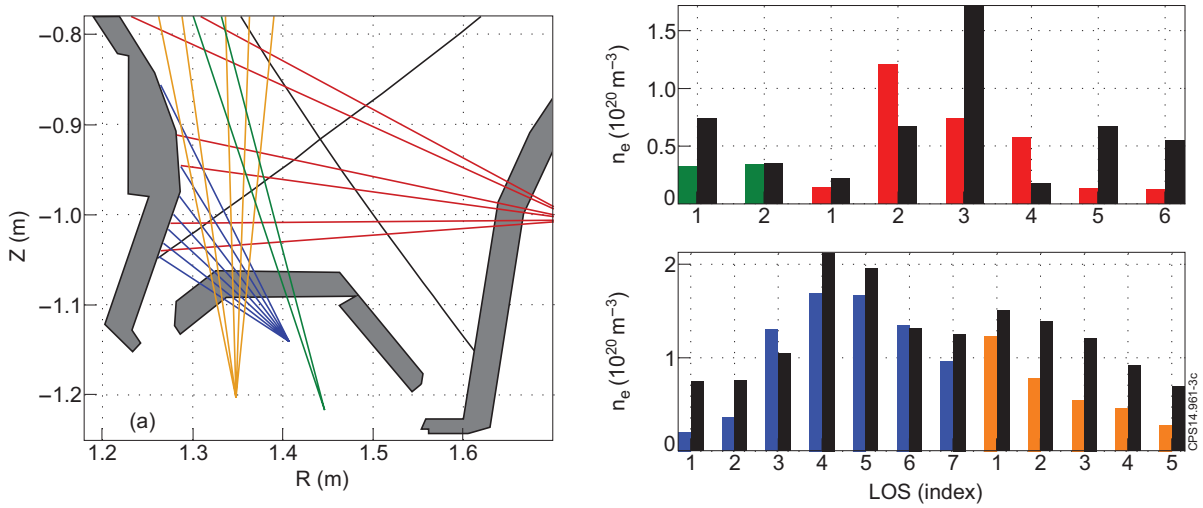

Figure 3: Geometry of the spectroscopic lines of sight in the divertor of ASDEX Upgrade in Pulse No: 27981 (left). Figures on the right show the comparison between the measured (black) and modelled electron densities along the LOS (colours corresponding to the LOS), as deduced from the Stark broadening of the D line [16]. The LOS indexes run from bottom to top (blue and red) and from left to right (green and yellow). The experimental data is from Pulse No: 27981 in the time range 2.7–2.8s, corresponding to the conditions in Pulse No: 27691.

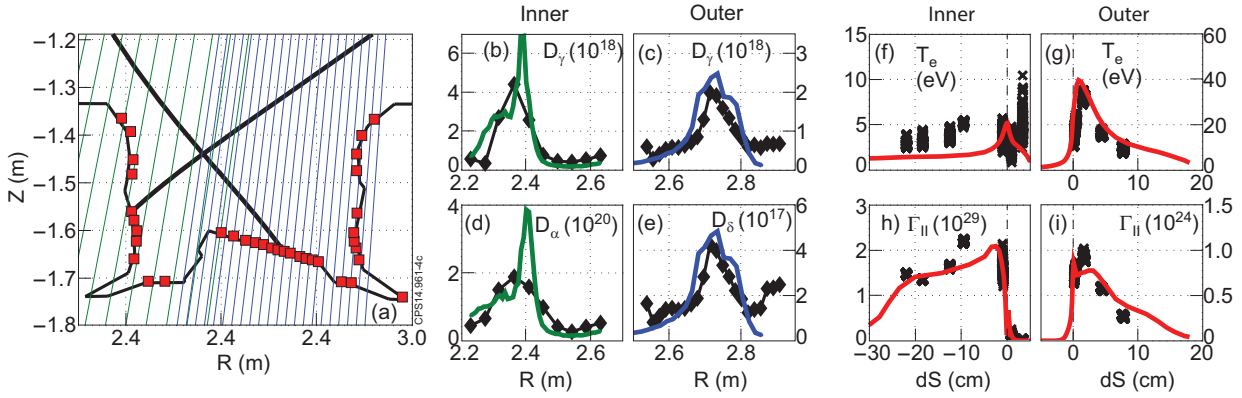

Figure 4: Divertor probe geometry and spectroscopic lines of sight in JET Pulse No: 82291 (a). Comparison between the simulated (coloured lines) and measured profiles (black markers) is shown in figures (b)-(i). Figures (b),(d) and (c),(e) show the spectroscopic measurements (in units [Ph/sr/m^2/s]) in the inner and outer divertor, respectively. Figures (f),(h) and (g),(i) show the Langmuir probe measurements T_e [eV] and Γ [$m^{-2}s^{-1}$] at the inner and outer target, respectively.

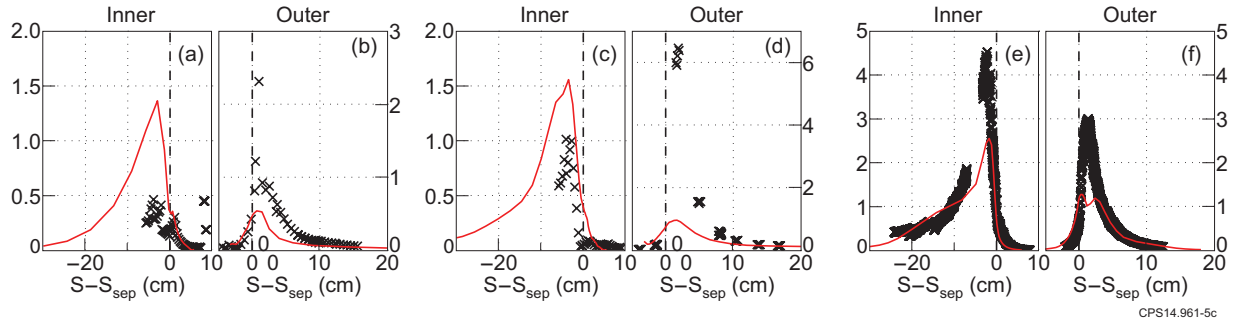

Figure 5: Modelled (red lines) and measured ion fluxes (black markers) along the two divertor targets in the ASDEX Upgrade Pulse No: 27688 (a)-(b) and Pulse No: 28818 (c)-(d) and in the JET Pulse No: 82295 (e)-(f). The units are [10^{24} $m^{-2}s^{-1}$].